JN-00957-2004: Final Accepted Version

Title:

Slow and fast inhibition and an h-current interact to create a theta rhythm in a model of CA1 interneuron network.

Authors:

Horacio G. Rotstein[1], Dmitri D. Pervouchine[1], Corey D. Acker[3], Martin J. Gillies[2], John A. White[3], Eberhardt H. Buhl[4], Miles A. Whittington[2] and Nancy Kopell[1]

Affiliations:

[1] Department of Mathematics and Statistics and Center for Biodynamics, Boston University, Boston, MA, 02215, USA.

[2] School of Biomedical Sciences, University of Leeds, Leeds LS2 9NQ, UK.

[3] Department of Biomedical Engineering and Center for Biodynamics, Boston University, Boston, MA, 02215, USA.

[4] Deceased.

Running head:

Theta rhythm in a model of CA1 interneuron network.

Contact information :

Horacio G. Rotstein

Department of Mathematics and Statistics and Center for Biodynamics,

Boston University

Boston, MA, 02215

E-mail: horacio@math.bu.edu

Phone: 617 353 1493 fax: 617 353 8100

In memory of Eberhardt H. Buhl

Key words: Hippocampus, Hodgkin-Huxley, hyperpolarization-activated current, oriens-lacunosum moleculare, synchronization

Abstract:

The Oriens-lacunosum moleculare (O-LM) subtype of interneuron is a key component in the formation of the theta rhythm (8 - 12 Hz) in the hippocampus. It is known that the CA1 region of the hippocampus can produce theta rhythms *in vitro* with all ionotropic excitation blocked, but the mechanisms by which this rhythmicity happens were previously unknown. Here we present a model suggesting that individual O-LM cells, by themselves, are capable of producing a single-cell theta -frequency firing, but coupled O-LM cells are not capable of producing a coherent population theta. By including in the model fast spiking (FS) interneurons, which give rise to IPSPs that decay faster than those of the O-LM cells, coherent theta rhythms are produced. The inhibition to O-LM cells from the FS cells, synchronizes the O-LM cells, but only when the FS cells themselves fire at a theta (or roughly multiple) frequency. Reciprocal connections from the O-LM cells to the FS cells serve to parse the FS cell firing into theta bursts, which can then synchronize the O-LM cells. A feature of the model O-LM cell critical to the synchronization mechanism is the hyperpolarization-activated h-current. The model can robustly reproduce relative phases of theta frequency activity in O-LM and FS cells.

INTRODUCTION

Field potential oscillations at theta frequencies (8-12 Hz) in the hippocampal formation have been correlated with various brain functions and behavioral states, including representation of visuospatial information (O'Keefe & Nadel 1978; O'Keefe & Recce 1993; Skaggs *et al.* 1996; Kahana *et al.* 1999), REM sleep (Jouvet 1969), active exploration (Vanderwolf 1969), and memory formation and retrieval (Larson & Lynch 1986; Buzsáki 1989; Lisman & Idiart 1995; Raghavachari *et al.* 2001). The theta rhythm is most regular in frequency and largest in amplitude in the stratum lacunosum-moleculare of the hippocampal CA1 region (Buzsáki 2002) (and references therein).

There are at least two forms of theta, both dependent on the medial septum *in vivo*: an atropine-sensitive form (presumably requiring a cholinergic input from the septum), and an atropine-resistant form, dependent on the entorhinal cortex and probably requiring NMDA receptors (Buzsáki *et al.* 1983). Though *in vivo* lesions of major input regions for the hippocampus and entorhinal cortex have profound effects on hippocampal/ entorhinal theta (Buzsáki *et al.* 1983; Lee *et al.* 1994), this does not imply that these regions are the only source of the theta rhythm. In addition to imposition of theta rhythms on the hippocampus by the septum and the entorhinal cortex, there are a variety of dynamical mechanisms intrinsic to the hippocampal formation that allow networks to create or resonate to rhythms in that frequency range, possibly with anatomically separate generators of similar rhythms (Kocsis *et al.* 1999; Csisvari *et al.* 2003).

The entorhinal cortex (EC), CA1 and CA3 all have cells that are capable of producing oscillations in the theta-frequency regime. The EC has excitatory spiny stellate cells, which are also able to generate single-cell theta oscillations (Alonso & Llinás 1989). CA1 and CA3 have a variety of inhibitory cell-types believed to be able to produce single-cell oscillations (Chapman & Lacaille 1999a,b; Banks *et al.* 2000; White *et al.* 2000b; Gillies *et al.* 2002). Under the appropriate pharmacological circumstances, hippocampal brain slices generate synchronized activity at theta frequencies (Gillies *et al.* 2002; Konopacki *et al.* 1987; Fellous & Sejnowski 2000; Williams & Kauer 1997).

Of particular interest for this paper is the work of Gillies *et al.* (2002) concerning an atropine-resistant theta produced in an *in vitro* model (CA1). In their experiments they used metabotropic receptor activation combined with AMPA receptors blockade, which suppresses gamma oscillations that would otherwise occur (Gillies *et al.* 2002). This work demonstrated a theta rhythm generated by the internal circuitry within area CA1 alone. The profile of the theta rhythms seen bore a number of similarities to theta rhythms seen *in vivo* involving: (1) A sharp phase reversal in mid stratum radiatum was seen (Buzsáki *et al.* 1986). (2) Pyramidal cell spike timing and rates with reference to the field theta rhythm and a distinct pattern of spike timings for fast spiking and oriens-lacunosum moleculare (O-LM) interneurons (Fox *et al.* 1986; Bragin *et al.* 1995; Harris *et al.* 2000). (3) Dendritic electrogenesis in pyramidal cells (Kamondi *et al.* 1998). The study by Gillies *et al.* (2002) implicated O-LM cells as critical for the theta rhythm gener-

ated internally within area CA1. These cells have a strong intrinsic theta rhythm (Maccaferri & McBain 1996; Saraga *et al.* 2003) which leads to them generating theta frequency outputs during field gamma rhythms as well as in theta models (Gillies *et al.* 2002; Gloveli *et al.* 2005). The outputs from these cells, whose bodies are in stratum oriens, are projected as slow inhibitory postsynaptic potentials onto the distal dendrites of pyramidal neurons (Whittington & Traub 2003). O-LM cells also have axonal projections to the lacunosum moleculare layer, and some axon collatorals in the stratum oriens (Hájos & Mody 1997); the latter provide an anatomical substrate for synaptic connections among O-LM cells.

The purpose of this paper is to examine the biophysical mechanism of production of the coherent theta oscillations in the *in vitro* CA1 preparation. Thus, we are concerned with both the intrinsic properties of the interneurons and the dynamical mechanisms that create coherence. In the data of Gillies et al. (2002) cells do not fire in absolute synchrony. Rather, there is a loose pattern of spikes of different kinds of interneurons (shown in Fig. 4**A**, to be discussed below), which we call "ragged synchronization". We shall show that the mechanism we propose can account for details of this loose coherence. The results of the paper depend critically on the slow, hyperpolarization-activated mixed cation current I_h, known to be expressed in O-LM cells (Gillies *et al.* 2002; Saraga *et al.* 2003). This current is important because it changes the synchronization properties of the cells that express it (Acker *et al.* 2003; Rotstein *et al.* 2005; Crook *et al.* 1998): while models of cells with only simple spiking currents synchronize well with inhibition, but not

excitation, the opposite is true when model cells express certain slow currents, including I_h (Acker *et al.* 2003; Rotstein *et al.* 2005; Crook *et al.* 1998). I_h is also important because it changes the response of the cell to inhibition: instead of delaying spikes, the inhibition can cause spikes to arrive faster. In the network of O-LM and fast-spiking interneurons we investigate, both effects of I_h play a large role.

METHODS

Experimental

Transverse hippocampal slice (450 μm) were prepared from adult Wistar rats, anaesthetized with inhaled isoflurane, immediately followed by an I.M. injection of ketamine ($\geq$ 100 mg kg^{-1}) and xylazine ($\geq$ 10 mg kg^{-1}) and transferred to a recording chamber. Here, they were maintained at 34 ^{o}C at the interface between a continuous stream (1.2ml/min) of ACSF (composition in mM: NaCl (126), KCl (3), NaH_2PO_4 (1.25), $NaHCO_3$ (24), $MgSO_4$ (2), $CaCl_2$ (2) and glucose (10)), and warm, moist carbogen gas (95% O2 : 5% CO_2). Slices were permitted to equilibrate for 45 minutes before any recordings commenced. Theta oscillations in area CA1 were induced by bath application of DHPG ((S)-3,5-dihydroxyphenylglycine) 60 μM and NBQX (2,3-dioxo-6-nitro-1,2,3,4-tetrehydrobenzo[f]quinoxaline-7-sulfonamide) 20 μM, both from Tocris, UK. Extracellular recording of theta activity were taken from stratum pyramidale using glass electrodes filled with ACSF (resistance 2-5 MΩ).

Intracellular recordings from somata of pyramidal neurons and FS interneurons with cell bodies in stratum pyramidale were taken with glass electrodes filled with KCH_3SO_4 (resistance 70-130 MΩ).

Computational

The inhibitory network studied in this paper consists of N_O O-LM (O-) cells and N_I fast spiking interneurons (I-cells). Each cell is modeled using the conductance-based Hodgkin-Huxley (HH) formalism. The dynamic equations are given in the Appendix. Both the O- and I-cells are described as one compartment having standard HH currents (transient Na, delayed rectifier K and leak). For the O-cells, the modeling also incorporates a hyperpolarization activated current I_h with 2 components (slow and fast kinetics) and an additional current I_p which is active during the interspike interval. The parameter range is chosen so that the h-current is necessary for an isolated O-cell to spike as occurs in the experiments described in (Gillies *et al.* 2002). The extra current I_p is modeled as the persistent sodium current in models of entorhinal spiny stellate cells (Acker *et al.* 2003). Spontaneous firing of O-neurons is known to occur at $\sim 5-20$ Hz. (Lacaille *et al.* 1987; Maccaferri & McBain 1996; Ali & Thomson 1998; Saraga *et al.* 2003). In most of the simulations presented here we follow (Saraga *et al.* 2003) and choose the natural frequency of the O-cells (i.e. the frequency in absence of synaptic inputs) to be ~ 12 Hz. However, these results are robust to changes in these natural frequencies. The cells are synaptically connected with IPSPs from

O-cells lasting longer than those originating from I-cells. The decay times of O and I IPSPs (defined as the time it takes for the synaptic conductance to decrease to $\sim 37\%$ of its maximum value) are 20 ms and 10 ms respectively (Traub *et al.* 1996; Hájos & Mody 1997). For the former there are no measurements of O-I IPSPs, and the 20 ms number we use for most of the simulations is taken from O to pyramidal cells connections; other values are investigated and discussed.

We consider all possible putative connectivity among the I-cells and O-cells. Some evidence for I-O and O-I connections are in the results section. O-O connections have not been found experimentally. As we show, the O-O connections, if present, do not help synchronization at theta frequencies for biologically plausible values of the parameters.

The network is globally connected (all-to-all connections) with heterogeneous synaptic connectivity. We create a spatial structure by ordering the cells as schematically shown in Fig. 4**C**. In our simulations the maximal synaptic conductances are larger the closer the cells in the network (see Appendix). In Fig. 4**C** this heterogeneity is schematically represented by the thickness of the connections: the thicker the line, the stronger the connection; for O-O and I-I we show only the strongest connections. Note that for cells far enough apart, the synaptic connectivity may be close to zero. I-cells have autapses in order to account for some network inhibitory effects.

Large network simulations are performed using custom software implemented in Matlab and C using Matlabs application program interface (mex). This software is a flexible tool to rapidly simulate scalable networks of model

neurons with easily variable network structure and connectivity. Numerical integration is performed in C using a standard adaptive step-size Runge-Kutta algorithm. Synapses are implemented using an efficient algorithm that affords tremendous improvements in simulation times for networks of single-compartment neurons (Lytton 1996). Small network simulations are performed using a Runge Kutta method of order four (Burden & Faires 1980) and the XPP software (Ermentrout 2002).

RESULTS

A network of O-cells does not create a coherent theta rhythm

Fig. 1 shows an example of the firing when a pair of O-cells (Fig. 1**A**) is coupled via inhibition. For each of two levels of coupling, antiphase patterns are formed (Fig. 1**B**). Note that the period of the network decreases with the increase in coupling conductance. These results are robust for a large range of coupling strengths, natural frequencies of O-cells and initial conditions. For initial conditions very close to synchrony, the cells do synchronize. However, that range of initial conditions is very small, and essentially disappears when the coupling conductance G_{OO} is set to at least 0.1 (Fig. 1**C**). As the number of cells in the O-network increases, the probability of finding all cells in the small basin of attraction of in-phase synchrony decreases, so for cells initially in splay-phase two antiphase clusters are found (data not shown). Thus,

with just O-LM cells in the network, synchrony is not robust. Though the network can robustly produce rhythms, when there is anti-phase or clusters, the population frequency is higher than theta for physiological values of the parameters.

The non-synchronization results persist when gap junctions are added, even with a gap junctional conductance large enough that the electrical coupling current during a spike is the same order of magnitude as the maximal inhibitory coupling current (data not shown).

Input from I-cells can sometimes synchronize O-cells

It is known that common inhibition can create synchrony (Wang & Rinzel 1992; van Vreeswijk *et al.* 1994; Gerstner *et al.* 1996; White *et al.* 1998; Chow *et al.* 1998). Fig. 2**A** contains evidence that O-cells receive fast inhibition, presumably from the I-cells. In a network of I and O-cells (Fig. 2**B**), the inhibition from the I-cells can indeed help to synchronize the O-cells. However, because of the hyperpolarization-activated current in the O-cells, the effect of inhibition on the O-cells is not straightforward: it depends on the frequency of the I-cell input, which interacts with the time scales of the I_h current. Some effects are shown below in Fig. 2; a more detailed mathematical treatment of these effects is in progress.

Fig. 2**C** shows the network when a pair of O-cells starting in anti-phase receives common inhibition at 8 Hz with the O-cells connected with $G_{OO} = 0.01$ (the results still hold with $G_{OO} = 0$). Note that the I-cell inhibition

leads quickly to synchronization of the O-cells. This is true for input up to 13 Hz (with these parameters). The last panel shows the conductance of the h-current of each of the two O-cells. Note that the conductance increases quickly as the pulse of inhibition is received, and drops quickly right after the cell spikes.

The input from I-cells at higher frequencies (13-30 Hz), however, is fast enough to suppress some of the O-cell spikes. In this range of frequencies, the natural driving currents of the cell cannot withstand the inhibition. However, the hyperpolarization-activated current I_h comes into play. Each time there is a pulse of inhibition, this current builds up, until the cell fires (Kopell & LeMasson 1994). However, the O-cells may phase-lock to different cycles of the input from I-cells. This results in a pattern with a constant phase lag between the O cells; the phase lag can be zero, if the cells start with very close initial conditions, but for more generic initial conditions the pattern is phase-locked rather than synchronous. Fig. 2**D** shows this for an I-cell firing at $\sim$ 28 Hz and imposing a coherent but not synchronous $\sim$ 8 Hz pattern on the O-cells. The last panel of this figure shows the time course of I_h in two O-cells. At still higher input frequencies (above $\sim$ 28 Hz), the process of the build up of I_h may take many more cycles, and if the input frequency is sufficiently high, the O-cells may be completely suppressed (data not shown).

To summarize, at input frequencies starting from not much above that in the uncoupled O-cell, the inhibitory input may create synchrony in the O-cells, but not in a way robust to changes in input frequency or initial conditions. This is important since the frequency of the I-cell may go up to

70 Hz (Buzsáki & Chrobak 1995).

Feedback from O to I-cells creates a more robust theta rhythm

Evidence for slow IPSPs onto I-cells is given in Fig. 3**A**. Though the O-cells produce such slow IPSPs (Gillies *et al.* 2002) it has not yet been experimentally shown that the IPSPs in Fig. 3**A** come from the O-cells. We hypothesize that they do.

The effects of the O $\rightarrow$ I feedback (Fig. 3**B**) depend on the strength of the feedback and the frequency. We focus on the parameter range in which the O $\rightarrow$ I coupling is not strong enough to suppress the spikes of the I-cells. If the I-cell firing is already in the theta range (without feedback), the input from the I-cells already synchronizes the O-cells, as shown above (Fig. 2). With feedback, that situation applies for some higher natural frequencies of the I-cells, since the O $\rightarrow$ I coupling slows downs the I-cells. This is shown in Fig. 3**C** for natural frequency of the I-cell at 13 Hz that has slowed down to 9 Hz by the inhibitory feedback from the O-cells.

At the higher natural frequencies of the I-cell, the central effect of the feedback is to cluster the I-cell spikes into theta frequencies. This is shown in Fig. 3**D**. As the natural frequency of the I-cell gets higher, the number of I-cell spikes per theta cycle increases (data not shown). Thus the local I-cell frequency can be in the high gamma range while still showing theta-frequency modulation that makes it effective in synchronizing O-cells.

Heterogeneity in connections and I_h creates a ragged theta rhythm

In Fig. 4**A**, data from (Gillies *et al.* 2002), we see overlaid traces from nine consecutive theta periods ($\sim$ 8 Hz.) aligned with the peak upward deflection in concurrently recorded stratum pyramidale field potentials. The top panel corresponds to the stratum pyramidale interneurons (I), the middle panel corresponds to the stratum oriens (O) interneurons and the bottom panel to the stratum pyramidale field. O-cells generate single action potentials (AP) on the initial rising phase of the field theta oscillations, while I-cells generate bursts of action potentials during the descending phase of the field theta oscillation. The superimposed traces show a consistent pattern of activity that was obtained for different O- and I-cells in several experiments: At the beginning of each theta cycle I-cells fire a large number of APs. This number decreases as the cycle is advanced and I-cells are almost silent when O-cells start firing. After the O-cells stop firing there is an interval before I-cells start firing again.

In Fig. 4**C** we show a schematic large network (see methods for description and parameters) of I- and O-cells. Unlike the small networks described above, each O-cell is not connected with the same strength to each I-cell and vice versa, so cells receive different amounts of inhibition. A simulation of that network (Fig. 4**B**) reproduces all the main features of the data in Fig. 4**A**: I- and O-cells fire in consecutive and slightly overlapped subintervals of the theta cycle and there is a silent subinterval of the theta cycle between the

firing of O- and I-cells. Most AP activity in the I-cells is observed at the beginning of the theta cycle, and then the activity of I-cells decreases while the O-cells become active. We observed (not clearly seen in Fig. 4**B**) that each O-cell fires once per period while I-cells fire multiple APs. An important observation in Fig. 4**B** is that, as experimentally observed, each cell does not necessarily fire at the same phase relative to the theta cycle.

This result does not depend on the size of the network, and in fact can be reproduced in a network of 2 O-cells and 2 I-cells (Fig. 4**D**). Note that neither the I-cells nor the O-cells are completely synchronous. Furthermore, as in the data and the above simulation, the spiking of the I-cells overlaps that of the O-cells. The O-cells fire when the I_h current has built up enough via the I-cell input to spike, turning off the I-cells. The latter, without this current, must wait until the slower-decaying O-cell inhibition wears off. The overlap occurs because the O-cells do not have to wait until the I-cell firing ceases. The same arguments apply to the larger network.

Direct comparison of theta field potential oscillations in the present model was not possible. However, field potentials can be thought of as representative of the average sum of all synaptic inputs and intrinsic membrane potential changes in a local population of principal cells (E) around the recording electrode. To compare the E-cell somatic membrane potential of the experimental situation to our model, we added an E-cell, modeled in the same way as an I-cell; the E-cell received inhibition from the O- and I-cells. In (Fig. 4**E**) we show that in both model and experiment, individual theta periods began with a large IPSP. Superimposed on the late decay phase of this IPSP were

additional smaller IPSPs.

DISCUSSION

The goal of this paper is to illuminate the mechanistic basis for the generation of one version of a coherent theta rhythm. The first central result is that O-cells and $GABA_A$ mediated inhibition, with or without electrical coupling, cannot account for the experimentally observed coherence and dynamics. This result depends strongly on the slow, hyperpolarization-activation mixed cation current I_h, known to be expressed in O-cells (Gillies *et al.* 2002; Saraga *et al.* 2003). The second central result is that fast spiking perisomatic targeting (FS) interneurons, known to participate in ragged synchronization (Gillies *et al.* 2002) can robustly entrain and synchronize O-cells, but only if the I-cells are firing at rates in the theta (8-12 Hz) range. This result depends on the fact that O-cells generate so-called "rebound spikes" after recovering from inhibition. O-cells are synchronized by the rebound phenomenon, which depends critically on I_h. O-cells are not entrained, and not necessarily synchronized by fast (> 12 Hz) spike trains from I-cells. Our third central result is that feedback from O-cells to I-cells can regulate activity of I-cells to lie within the appropriate frequency range, allowing the network as a whole to generate coherent theta oscillations. Under the realistic assumption that connections within the network are not perfectly symmetric, this network of O- and I-cells generates "ragged synchronization" with phase relationships very similar to those seen in vitro. The network rhythm does

not depend on network size, and can be explained mechanistically in terms of the interactions of fast inhibition from I-cells, slow inhibition from O-cells, and the prominence of I_h in O-cells but not in I-cells.

Mechanism of coherent theta in in vitro CA1 preparation

Individual O-LM cells (O-cells) can produce a theta rhythm, but populations of them are not coherent at that frequency range. Indeed, the slow hyperpolarization-activated cation current I_h, which gives these cells their theta-rhythmic quality, is itself responsible for the lack of synchronization via mutual inhibition (see also Acker et al. 2003): when a cell expresses I_h, inhibition to that cell soon after it spikes leads to advances of the next spike, while later inhibition retards the next spike.

The result is that, if two cells start firing close to one another, the dynamics pushes the spike times further apart (Acker *et al.* 2003).

Addition of FS interneurons (I-cells) to the network produces coherence in the theta-frequency range, even though the I-cells themselves are capable of firing at higher frequencies, and in fact fire at average rates well above 12 Hz even during theta synchronization. Our simulations imply that two properties of O-cells are crucial for generating a coherent theta rhythm. First, they express I_h. This current allows them to generate "rebound" spikes after inhibition. The timing of the rebound spikes, in turn, leads to increased synchronization among O-cells receiving common input. Second, O-cells are

believed to give rise to slow GABAergic IPSPs postsynaptically (Gillies *et al.* 2002). These slow IPSPs make it easier for slowly rhythmic O-cells to impose a firing pattern on I-cells that includes significant pauses once per theta cycle. This firing pattern in I-cells is sufficient to induce the O-cells to spike synchronously via the h-current build-up mechanism described earlier. The pattern is precise for networks in which all O-cells receive identical projections from the I-cells, but realistically "ragged" when the projections from I-cells to O-cells are not uniform. The phenomenon is remarkably independent of network size.

One detail of both the experimental dynamics and the model provides an important clue to the role of I_h in the coherence mechanism: there is an overlap between the firing of the I-cells and the onset of firing of the O-cells. This overlap comes about because the I-cells not only suppress firing during some intervals, but they prime the O-cells to generate subsequent rebound spikes. Thus, the first set of I-cell spikes can activate the O-cells, and allow them to fire even while inhibition continues to arrive from the I-cells.

The model offered in this paper was able to reproduce subtle relative timing of the O-LM cells and I cells, as well as IPSP traces in E-cells (Fig. 4). The E-cell somatic membrane potential changes were remarkably similar in model and experiment. The only discrepancy was that, in the model, two additional small IPSPs were always seen, whereas in experiment the number of smaller IPSPs was variable, ranging from five to one. This could be explained by the relatively small size of the model network compared with the available network architecture in the *in vitro* slice preparation. By using

small networks, we were able to explain the origin of the theta coherence, via the properties of I_h and the two types of inhibition in the network.

Related literature

This paper deals only with interneuronal networks that produce a theta-frequency rhythm. There is also a substantial literature, both experimental and theoretical, dealing with gamma-frequency interneuronal networks (van Vreeswijk *et al.* 1994; Skinner *et al.* 1994; Gerstner *et al.* 1996; Jefferys *et al.* 1996; Traub *et al.* 1996; Wang & Buzsáki 1996; Chow *et al.* 1998; Buzsáki & Chrobak 1995; Bragin *et al.* 1995; White *et al.* 1998, 2000a; Tiesinga & Sejnowski 2004; Lytton *et al.* 1996). The gamma-frequency networks have different properties because of the absence of the h-current in the model cells; this current is important, though not critical, for the expression of a theta rhythm (Dickson *et al.* 2000b). The present paper extends the synchronization theory to cells that contain this ubiquitous current, and to network that contain such cells.

The model that we used for the O-cell is inspired by models of the stellate cells of the entorhinal cortex (Acker *et al.* 2003; Dickson *et al.* 2000a). For the stellate cells, the ability to produce subthreshold and spiking theta rhythms has been traced to a persistent Na current ($I_{Na,p}$), plus I_h and/or a slow outward K-current. In this paper, we did not use the extra K-current. The I_p current we use has dynamics similar to $I_{Na,p}$, but that is not essential; it can be replaced by other currents that are slow and inward, even a tonic

excitatory current. In keeping with our aim of understanding network dynamics using the simplest biophysically realistic model, our single compartment model of O-cells is less complex than the multi-compartment model used by Saraga et al. (2003) to simulate back-propagating action potentials in O-cells. We believe that the differences between these two models are not important for the major conclusions of this paper (Gloveli *et al.* 2005).

Modeling of stellate cells is consistent with the results for this model. It was shown (Acker *et al.* 2003) that models of such cells synchronize with excitation, but not with fast inhibition. As we show here, they do not synchronize with slow inhibition either. The novelty of the current work is in how the two kinds of inhibition work together to create a coherent rhythm.

A more complex model that includes the O-cells is in Kunec *et al.* (2005). That paper investigated a model with fast-spiking interneurons, O-cells and pyramidal cells, with external input from the medial septum, the dentate and the entorhinal cortex. The O-cells were shown to play an important role in separating the theta rhythm into an epoch in which inputs could lead to potentiation of synapses and an epoch in which the potentiated synapses could lead to firing of unstimulated neurons.

Further modeling issues

The current model does not explicitly include NMDA currents, even though Gillies *et al.* (2002) reported that block of NMDA receptors affects the *in vitro* theta rhythm. We hypothesize that this effect of the NMDA receptor

blockers is related to a feature of the NMDA receptors separate from their role in excitatory transmission: they play a role in reversing agonist-induced desensitization of mGluR5 (Alagarsamy *et al.* 1999b,a). Hippocampal neurons are sensitive to mGluR-dependent drive (Wang & Buzsáki 1996), and interactions between these and NMDA receptors have been reported (Awad *et al.* 2000; Luthi *et al.* 1994). In the current model, we keep the drive from mGluR receptors constant, implicitly using the NMDA effect of blocking desensitization. We do not use the kinetics of the NMDA currents; indeed, we do not use any EPSPs. This is consistent with the Gillies *et al.* (2002) findings, in which the pyramidal cells fire exceedingly sparsely. Our model requires this sparseness, since excitation from the NMDA receptors would otherwise deactivate the h-current of the O-cells necessary for the timing effects we have described.

The observation of rhythmic periods of quiescence in I-cells in experimental theta oscillations can be explained in the model entirely by input from O-cells. However, given that no direct quantification of O-cell input kinetics to I-cells is available we cannot rule out involvement of additional factors in the slice preparation or *in vivo*. We have used the kinetics associated with the O-cell inputs onto pyramidal cells; as shown in Fig. 4**E**, the model output is consistent with experimental data. We have more briefly investigated the effects of faster-decaying IPSPs from the O-cells. For O-O connections we found that IPSPs decaying at faster rates (down to 10 ms) create more robust antiphase solutions. We also considered O-O and O-I connections with much larger decay times (up to 40 ms) and found the results are robust

with minor changes in other parameters.

In vitro experiments in CA3 suggest that a somewhat different mechanism produces a theta rhythm in that region (Gillies *et al.* 2002). In CA1, large enough depolarization of the slice, without blockage of AMPA-mediated excitation, produced gamma rhythms, with a suppression of the theta rhythm. This is understandable from our current model (data not shown): when there are gamma oscillations, the I-cells fire at a gamma frequency, which, in our model, suppresses the O-cells (Netoff *et al.* 2004). In CA3, however, theta frequency oscillations were more prominent (compared to CA1) in the absence of AMPA receptor blockade, with a nested gamma/theta rhythm as in (Bragin *et al.* 1995; Leung 1998). When AMPA receptors were blocked (Gillies *et al.* 2002), both gamma and theta were attenuated. Though this was not the focus of the current paper, we are also able to reproduce that result in our model by modification of the tonic drive to the O- and I-cells: the simulations modeling the CA3 data have parameters tuned so that the O- and I-cells do not fire without phasic excitation. With AMPA mediated excitation, there is a theta rhythm nested with gamma (data not shown) (Rotstein *et al.* 2002).

Our simulations were designed to explain population activity observed in vitro, but it is important to note that atropine-resistant theta in slices is similar to its counterpart from *in vivo* recordings of neurons in urethane-anesthesized rats in CA1 (Klausberger *et al.* 2003). In both cases, FS interneurons fired preferentially (often more than one spike) on the descending phase of the extracellular theta oscillations recorded in the stratum pyrami-

dale, and O-cells fired rhythmically at the trough of the theta cycles. The similarities between the data derived from our mathematical model and that seen in experiments suggests that the interplay betwenn I_h and synaptic interactions between heterogeneous interneuron populations may constitute an important mechanism involved in population dynamics intrinsic to the hippocampus.

APPENDIX

The inhibitory network studied in this manuscript consists of N_O O-LM (O) cells and N_I FS (I) cells. In what follows $k = 1, \ldots, N_O$ and $j = 1, \ldots, N_I$. The current-balance equations for the O- and I- cells are

$$C_O \, dv_{O,k} \,/\, dt = I_{app,O} - I^k_{O,Na} - I^k_{O,K} - I^k_{O,L} - I^k_{O,p} - I^k_h - Isyn_{\,O,k},$$

and

$$C_I \, dv_{I,j} \,/\, dt = I_{app,I} - I^j_{I,Na} - I^j_{I,K} - I^j_{I,L} - Isyn_{\,I,j},$$

respectively, where $v_{O,k}$ and $v_{I,j}$ are the membrane potentials (mV), C_O and C_I are the membrane capacitances $(\mu F/cm^2)$, $I_{app,O}$ and $I_{app,I}$ are the applied bias (DC) current (μA), and the ionic and synaptic currents are given by

$I^k_{O,Na} = G_{O,Na} \, m^3_{O,k} \, h_{O,k} \, (v_{O,k} - E_{O,Na})$,

$I^k_{O,K} = G_{O,K} \, n^4_{O,k} \, (v_{O,k} - E_{O,K})$,

$I^k_{O,L} = G_{O,L} \, (v_{O,k} - E_{O,L})$,

$I^k_{O,p} = G_p \, p_{O,k} \, (v_{O,k} - E_{O,Na})$,

$I^k_{O,h} = G_h \, (\, 0.65 \, h^f_{O,k} + 0.35 \, h^s_{O,k} \,) \, (v_{O,k} - E_h)$,

$I^j_{I,Na} = G_{I,Na} \, m^3_{I,j} \, h_{I,j} \, (v_{I,j} - E_{I,Na})$,

$I^j_{I,K} = G_{I,j}\, n^4_{I,j}\, (v_{I,j} - E_{I,j})$,

$I^j_{I,L} = G_{I,L}\, (v_{I,j} - E_{I,L})$,

$Isyn_{\,O,k} = \sum_{i=1,i\neq k}^{N_O} G_{OO,i,k}\, S_{OO,i}\, (\, v_{O,k} - E_{in}\,) + \sum_{i=1}^{N_I} G_{IO,i,k}\, S_{IO,i}\, (\, v_{O,k} - E_{in}\,)$,

and

$Isyn_{\,I,j} = \sum_{i=1}^{N_O} G_{OI,i,j}\, S_{OI,i}\, (\, v_{I,j} - E_{in}\,) + \sum_{i=1}^{N_I} G_{II,i,j}\, S_{II,i}\, (\, v_{I,j} - E_{in}\,)$.

In the expressions for the different currents I_X, G_X are the maximal conductances (mS/cm^2) and E_X are the reversal potentials (mV). Units of time are ms. All the dynamics variables $x_{O,k} = m_{O,k},\ h_{O,k},\ n_{O,k},\ p_{O,k},\ h^f_{O,k},\ h^s_{O,k}$ obey a first order differential equation of the following form:

$$dx_{O,k} \,/\, dt = (x_{O,\infty}(v_{O,k}) - x_{O,k}) \,/\, \tau_{x_O}(v_{O,k}),$$

where

$$x_{O,\infty}(v_{O,k}) = \alpha_{x_O}(v_{O,k}) \,/\, (\alpha_{x_O}(v_{O,k}) + \beta_{x_O}(v_{O,k})),$$

$$\tau_{x_O}(v_{O,k}) = 1 \,/\, (\alpha_{x_O}(v_{O,k}) + \beta_{x_O}(v_{O,k})),$$

and

$\alpha_{m_O}(v) = -0.1\,(v+23) \,/\, (e^{-0.1\,(v+23)} - 1)$,

$\beta_{m_O}(v) = 4\, e^{-(v+48)/18}$,

$\alpha_{h_O}(v) = 0.07\, e^{-(v+37)\,/\,20}$,

$\beta_{h_O}(v) = 1 \,/\, (e^{-0.1\,(v+7)} + 1)$,

$\alpha_{n_O}(v) = -0.01\,(v+27) \,/\, (e^{-0.1\,(v+27)} - 1)$,

$\beta_{n_O}(v) = 0.125\, e^{-(v+37)/80}$,

$\alpha_{p_O}(v) = 1 \,/\, (0.15\,(1 + e^{-(v+38)/6.5}))$,

$\beta_{p_O}(v) = e^{-(v+38)/6.5} \,/\, (0.15\,(1 + e^{-(v+38)/6.5}))$,

$h^f_{O,\infty}(v_{O,k}) = 1 \,/\, (1 + e^{(v+79.2)/9.78})$,

$\tau_{h_O^f}(v_{O,k}) = 0.51 \,/\, (e^{(v-1.7)/10} + e^{-(v+340)/52}) + 1,$

$h^s_{O,\infty}(v_{O,k}) = 1 \,/\, (1 + e^{(v+2.83)/15.9})^{58},$

$\tau_{h^s_O}(v_{O,k}) = 5.6 \,/\, (e^{(v-1.7)/14} + e^{-(v+260)/43}) + 1.$

All the dynamic variables $x_{I,k} = m_{I,k}, h_{I,k}, n_{I,k}$ obey a first order differential equation of the following form:

$$dx_{I,k} \,/\, dt = (x_{I,\infty}(v_{I,k}) - x_{I,k}) \,/\, \tau_{x_I}(v_{I,k}),$$

where

$$x_{I,\infty}(v_{I,k}) = \alpha_{x_I}(v_{I,k}) \,/\, (\alpha_{x_I}(v_{I,k}) + \beta_{x_I}(v_{I,k})),$$

$$\tau_{x_I}(v_{I,k}) = 1 \,/\, (\alpha_{x_I}(v_{I,k}) + \beta_{x_I}(v_{I,k})),$$

and

$\alpha_{m,I}(v) = 0.32\,(54 + v) \,/\, (1 - e^{-(v+54)/4}),$

$\beta_{m,I}(v) = 0.28\,(v + 27) \,/\, (e^{(v+27)/5} - 1),$

$\alpha_{h,I}(v) = 0.128\, e^{-(50+v)/18},$

$\beta_{h,I}(v) = 4 \,/\, (1 + e^{-(v+27)/5}),$

$\alpha_{n,I}(v) = 0.032\,(v + 52) \,/\, (1 - e^{-(v+52)/5})$

$\beta_{n,I}(v) = 0.5\, e^{-(57+v)/40}$

The synaptic variables S_{XZ} $(X, Z = O, I)$ obey first order differential equations of the form:

$$dS_{XZ,k} \,/\, dt = NT_{XZ}(v_{X,k})\,(\,1 - S_{XZ,k}\,) - \beta_{XZ}\, S_{XZ,k},$$

where

$$NT_{XZ}(v) = \tfrac{\alpha_{XZ}}{2}\,(\,1 + \tanh((v - Vth_{XZ})/Vsl_{XZ})\,).$$

The values of the parameters used in our simulations are $E_{O,Na} = 55$, $E_{O,K} =$

-90, $E_h = -20$, $E_{O,L} = -65$, $G_{O,Na} = 52$, $G_{O,K} = 11$, $G_{O,L} = 0.5$, $G_{O,p} = 0.5$, $C_O = 1$, $E_{I,Na} = 50$, $E_{I,K} = -100$, $E_{I,L} = -67$, $G_{I,Na} = 100$, $G_{I,K} = 80$, $G_{I,L} = 0.1$, $G_h = 1.46$, $I_{app,O} = -1.8$, $I_{app,I} = 0.48$, $E_{in} = -80$, $\alpha_{OZ} = 5$, $\beta_{OZ} = 0.05$, when $Z = 0, I$, $\alpha_{IZ} = 15$, $\beta_{IZ} = 0.11$, when $Z = O, I, E$, $\alpha_{EZ} = 20$, $\beta_{EZ} = 0.12$, when $Z = O, I$, $Vth_{XZ} = 0$, $Vsl_{XZ} = 0.1$, when $X, Z = O, I$.

The synaptic maximal conductances are given by

$$G_{OO,ik} = \begin{cases} A_{OO} e^{-\gamma_{OO}(i-k)^2} & 1 \le i, k \le N_O, \\ 0 & \text{otherwise,} \end{cases}$$

$$G_{IO,jk} = \begin{cases} A_{IO} e^{-\gamma_{IO}(i-k)^2} & 1 \le i \le N_I, 1 \le k \le N_O, \\ 0 & \text{otherwise,} \end{cases}$$

$$G_{OI,jk} = \begin{cases} A_{OI} e^{-\gamma_{OI}(i-j)^2} & 1 \le i \le N_O, 1 \le j \le N_I, \\ 0 & \text{otherwise,} \end{cases}$$

$$G_{II,jk} = \begin{cases} A_{II} e^{-\gamma_{II}(i-j)^2} & 1 \le i, j \le N_I, \\ 0 & \text{otherwise.} \end{cases}$$

The dynamical model of the E-cell is identical to the one for the I-cell, with the exception of the synaptic variable, which was omitted because E-cell's output is not used in this paper.

ACKNOWLEDGMENTS

We are grateful to G. Buzsáki, E. Sivan and S. Epstein for reading earlier versions of this manuscript and helpful comments; and to G. Duffy for helping in doing some of the figures.

GRANTS

This work was partially supported by the Burroughs Wellcome Fund (HGR and NK), NIH, award number 5 R01 NS46058-02 as part of the NSF/NIH Collaborative Research in Computational Neuroscience Program (MAW, NK and HGR), the MRC, UK (MAW), the Wellcome Trust (MAW), NIH R01 NS34425 (JAW).

References

Acker, C. D., Kopell, N., & White, J. A. 2003. Synchronization of strongly coupled excitatory neurons: relating network behavior to biophysics. *Journal of Computational Neuroscience*, **15**, 71–90.

Alagarsamy, S., Rouse, S. T., Gereau IV, R. W., Heineman, S. F., Smith, Y., & Conn, P. J. 1999a. Activation of N-Methyl-D-Aspartate receptors reverses desensitization of metabotropic glutamate receptor, mGluR5, in native and recombinant systems. *Ann. N.Y. Acad. Sci.*, **868**, 526–530.

Alagarsamy, S., Marino, M. J., Rouse, S. T., Gereau IV, R. W., Heinemann, S. F., & Conn, P. J. 1999b. Activation of NMDA receptors reverses desensitization of mGluR5 in native and recombinant systems. *NATURE Neurosci.*, **2**, 234–240.

Ali, A., & Thomson, A. 1998. Facilitating pyramid to horizontal oriens-alveus interneurone inputs: dual intracellular recordings in slices of rat hippocampus. *J Physiol*, **507**, 185–199.

Alonso, A. A., & Llinás, R. R. 1989. Subthreshold Na^+-dependent theta like rhythmicity in stellate cells of entorhinal cortex layer II. *NATURE*, **342**, 175–177.

Awad, H., Hubert, G. W., Smith, Y., Levey, A. I., & Conn, P. J. 2000. Activation of metabotropic glutamate receptor 5 has direct excitatory effects

and potentiates NMDA receptor currents in neurons of the subthalamic nucleus. *J. Neurosci.*, **20**, 7871–7879.

Banks, M. I., White, J. A., & Pearce, R. A. 2000. Interactions between distinct GABA(A) circuits in hippocampus. *NEURON*, **25**, 449–457.

Bland, B. H., & Colom, L. V. 1993. Extrinsic and intrinsic properties underlying oscillation and synchrony in limbic cortex. *Prog. Neurobiol.*, **41**, 157–208.

Bragin, A., Jando, G., Nadasdy, Z., Hetke, J., Wise, K., & Buzsáki, G. 1995. Gamma (40-100 Hz) oscillation in the hippocampus of the behaving rat. *J. Neurosci.*, **15**, 47–60.

Burden, R. L., & Faires, J. D. 1980. *Numerical analysis*. PWS Publishing Company - Boston.

Buzsáki, G. 1989. Two-stage model of memory trace formation: a role for 'noisy' brain states. *Neuroscience*, **31**, 551–570.

Buzsáki, G. 2002. Theta oscillations in the hippocampus. *NEURON*, **33**, 325–340.

Buzsáki, G., & Chrobak, J.J. 1995. Temporal structure in spatially organized neuronal ensembles: a role for interneuronal networks. *Curr. Opin. Neurobiol.*, **5**, 504–510.

Buzsáki, G., Czopf, J., Kondakor, I. & Kellenyi, L. 1986. Laminar distribution of hippocampal rhythmic slow activity (RSA) in the behaving rat:

Current source density analysis, effects of urethane and atropine. *Brain Res.*, **365**, 125–137.

Buzsáki, G., Leung, L. W., & Vanderwolf, C. H. 1983. Cellular bases of hippocampal EEG in the behaving rat. *Brain Res.*, **287**, 139–171.

Chapman, C. A., & Lacaille, J. C. 1999a. Cholinergic induction of theta-frequency oscillations in hippocampal inhibitory interneurons and pacing of pyramidal cell firing. *J. Neurosci.*, **19**, 8637–8645.

Chapman, C. A., & Lacaille, J. C. 1999b. Intrinsic theta-frequency membrane potential oscillations in hippocampal CA1 interneurons of stratum lacunosum-moleculare. *J. Neurophysiol.*, **81**, 1296–1307.

Chow, C. C., White, J. A., Ritt, J., & Kopell, N. 1998. Frequency control in synchronous networks of inhibitory neurons. *Journal of Computational Neuroscience*, **5**, 407–420.

Crook, S. M., Ermentrout, G. B & Bower, J. M. 1998. Spike frequency adaptation affects the synchronization properties of networks of cortical oscillations. *Neural Comput.*, **10**, 837–854.

Csisvari, J., Jamieson, B., Wise, K. D., & Buzsáki, G. 2003. Mechanisms of gamma oscillations in the hippocampus of the behaving rat. *NEURON*, **37**, 311–322.

Dickson, C. T., Magistretti, J., Shalinsky, M. H, Fransén, E., Hasselmo, M., & Alonso, A. A. 2000. Properties and role of I_h in the pacing of subthresh-

old oscillation in entorhinal cortex layer II neurons. *J. Neurophysiol.*, **83**, 2562–2579.

Dickson, C. T., Magistretti, J., Shalinsky, M. H, Hamam, B. & Alonso, A. A. 2000. Oscillatory activity in entorhinal neurons and circuits. *Ann. N.Y. Acac. Sci.*, **911**, 127–150.

Ermentrout, B. 2002. *Simulating, analyzing, and animating dynamical systems. A guide to XPPAUT for researchers and students.* Society for Industrial and Applied Mathematics.

Fellous, J. M., & Sejnowski, T. J. 2000. Cholinergic induction of oscillations in the hippocampal slice in the slow (0.5-2 Hz), theta (5-12 Hz), and gamma (25-70 Hz) bands. *Hippocampus*, **10**, 187–197.

Fox, S. E., Wolfson, S., & Ranck, J. B. J. 1986. Hippocampal theta rhythm and the firing of neurons in walking and urethane anesthetized rats. *Exp. Brain Res.*, **62**, 495–508.

Gerstner, W., van Hemmen, J. L., & Cowen, J. 1996. What matters in neuronal locking? *Neural Computat.*, **8**, 1653–1676.

Gillies, M. J., Traub, R. D., LeBeau, F. E. N., Davies, C. H., Gloveli, T., Buhl, E. H., & Whittington, M. A. 2002. A model of atropine-resistant theta oscillations in rat hippocampal area CA1. *J Physiol*, **543.3**, 779–793.

Gloveli, T., Dugladze, T., Saha, S., Monyer, H., Heinemann, U., Traub, R. D., Whittington, M. & Buhl, E. 2005. Differential involvement of

oriens/pyramidale interneurons in hippocampal oscillations *in vitro*. *J. Physiol.*, **562**, 131–147.

Gloveli, T., Dugladze, T., Rotstein, H. G., Traub, R. D., Monyer, H., Heinemann, U., Whittington, M. & Kopell, N. 2005. Orthogonal arrangement of rhythm generating microcircuits in the hippocampus. *In revision.*

Hájos, N., & Mody, I. 1997. Synaptic communication among hippocampal interneurons: properties of spontaneous IPSCs in morphologically identified cells. *J. Neurosci.*, **17**, 8427–8442.

Harris, K. D., Henze, D. A., Csicsvari, J., Hirase, H. & Buzsáki, G. 2000. Accuracy of tetrode spike separation as determined by simultaneous intracellular and extracellular measurements. *J. Neurophysiol.*, **84**, 401–414.

Hoppensteadt, F. C., & Izhikevitch, E. M. 1997. *Weakly Connected Neural Networks.* Springer-Verlag, NY.

Jefferys, J., Traub, R., & Whittington, M. 1996. Neuronal networks for induced '40 Hz' rhythms. *Trends Neurosci.*, **19**, 202–208.

Jouvet, M. 1969. Biogenic amines and the states of sleep. *Science*, **163**, 32–41.

Kahana, M. J., Sekuler, R., Caplan, J. B., Kirschen, M., & Madsen, J. R. 1999. Human theta oscillations exhibit task dependence during virtual maze navigation. *NATURE*, **399**, 781–784.

Kamondi, A., Acsady, L., Wang, X. J., & Buzsáki, G. 1998. Theta oscillations in somata and dendrites of hippocampal pyramidal cells in vivo: activity-dependent phase-precesion of action potentials. *Hippocampus*, **8**, 244–261.

Klausberger, T., Magill, P. J., Márton, L. F., Roberts, J. D. B., Cobden, P. M., Buzsáki, g., & Somogyi, P. 2003. Brain-state- and cell-type-specific firing of hippocampal interneurons *in vivo*. *NATURE*, **421**, 844–848.

Kocsis, B., Bragin, A., & Buzsáki, G. 1999. Interdependence of multiple theta generators in the hippocampus: a partial coherence analysis. *J. Neurosci.*, **19**, 6200–6212.

Konopacki, J., Bland, B. H., MacIver, M. B., & Roth, S. H. 1987. Cholinergic theta rhythm in transected hippocampal slices: independent CA1 and dentate generators. *Brain Res.*, **436**, 217–222.

Kopell, N., & LeMasson, G. 1994. Rhythmogenesis, amplitude modulation, and multiplexing in a cortical architecture. *Proc. Natl. Acad. Sci. USA*, **91**, 10586–10590.

Kunec, S., Hasselmo, M., & Kopell, N. 2005. Encoding and retrieval in the CA3 region of the hippocampus: a model of theta phase separation. *J. Neurophysiol.*, **In press**.

Lacaille, J.-C., Williams, S., Kunkel, D, & Schwartzkroin, P. 1987. Local circuit interactions between oriens/alveus interneurons and CA1 pyramidal cells in hippocampal slices: eletrophysiology and morphology. *J. Neurosci.*, **7**, 1979–1993.

Larson, J., & Lynch, G. 1986. Induction of synaptic potentiation in hippocampus by patterned stimulation involves two events. *Science*, **232**, 985–988.

Lee, M. G., Chrobak, J. J., Sik, A., Wiley, R. G., & Buzsáki, G. 1994. Hippocampal theta activity following selective lesion of the septal cholinergic system. **62**, 1033–1047.

Leung, L. S. 1998. Generation of theta and gamma rhythms in the hippocampus. *Neurosci. Biobehav. Rev*, **22**, 275–290.

Lisman, J. E., & Idiart, J. A. 1995. Storage of 7 ± 2 short term memories in oscillatory subcycles. *Science*, **267**, 1512–1515.

LoFaro, T., & Kopell, N. 1999. Timing regulation in a network reduced from voltage-gated equations to a one-dimensional map. *J. Math. Biol.*, **38**, 479–533.

Luthi, A., Gahwiler, B. H., & Gerber, U. 1994. Potentiation of a metabotropic glutamatergic response following NMDA receptor activation in rat hippocampus. *Pflugers Arch.*, **427**, 197–202.

Lytton, W. W. 1996. Optimizing synaptic conductance calculation for network simulations. *Neural Computat.*, **8(3)**, 501–509.

Lytton, W. W., Destexhe, A., & Sejnowski, T. J. 1996. Control of slow oscillations in the thalamocortical neuron: A computer model. *Neuroscience*, **70**, 674–684.

Maccaferri, G., & McBain, C. 1996. The hyperpolarization-activated current (I_h) and its contribution to pacemaker activity in rat CA1 hippocampal stratum oriens-alveus interneurones. *J Physiol*, **497**, 119–130.

Nadim, F., Manor, Y., Kopell, N., & Marder, E. 1999. Synaptic depression creates a switch that controls the frequency of an oscillator circuit. *Proc. Natl. Acad. Sci. USA*, **96**, 8206–8211.

Netoff, T.I., Pervouchine, D., Kopell, N, & White, J.A. 2004. Oscillation frequency switches in model and hybrid networks of the hippocampus. *Society for Neuroscience Abstracts. *32*, In press.*

O'Keefe, J. 1993. Hippocampus, theta, and spatial memory. *Curr. Opin. Neurobiol*, **3**, 917–924.

O'Keefe, J., & Nadel, L. 1978. *The Hippocampus as a cognitive map*. Clarendon, Oxford.

O'Keefe, J., & Recce, M. L. 1993. Phase relationship between hippocampal place units and the EEG theta rhythm. *Hippocampus*, **3**, 317–330.

Raghavachari, S., Kahana, J. J., Rizzuto, D. S., Caplan, J. B., Kirschen, M. P., Bourgeois, M., Madsen, J. R., & Lisman, J. E. 2001. Gating of human theta oscillations by a working memory task. *J. Neurosci.*, **21**, 3175–3183.

Rotstein, H. G., Gillies, J. A., Whittington, M. A., Buhl, E. H., & Kopell,

N. 2002. A model of an inhibition-based atropine-resistant theta frequency oscillation in CA1 in vitro. *Society for Neuroscience Abstracts*, **753.10**.

Rotstein, H. G., Gillies, M. J., Acker, C. D., White, J. A., Whittington, M. A., & Kopell, N. 2003. Slow and fast inhibition and h-current interact to create a theta rhythm in CA1. *Society for Neuroscience Abstracts*, **258.3**.

Rotstein, H. G., Oppermann, T., White, J. A. & Kopell, N. 2005. A reduced model for medial entorhinal cortex stellate cells: subthreshold oscillations, spiking and synchronization. *In revision.*

Saraga, F., Wu, C. P., Zhang, L., & Skinner, F. K. 2003. Active dendrites and spike propagation in multi-compartment models of oriens-lacunosum/moleculare hippocampal interneurons. *J Physiol*, **552.3**, 502–509.

Skaggs, W. E., McNaughton, B. L., Wilson, M. A., & Barnes, C. A. 1996. Theta phase precession in hippocampal neuronal populations and the compression of temporal sequencies. *Hippocampus*, **6**, 149–172.

Skinner, F. K., Kopell, N., & Marder, E. 1994. Mechanisms for oscillations and frequency control in networks of mutually inhibitory relaxation oscillators. *Journal of Computational Neuroscience*, **69-87**.

Squire, L. R., & Zola-Morgan, S. 1991. The medial temporal lobe memory system. *Science*, **253**, 1380–1386.

Stewart, M., & Fox, S. E. 1990. Do septal neurons pace the hippocampal theta rhythm? *Trends Neurosci.*, **13**, 163–168.

Tiesinga, P. H., & Sejnowski, T. J. 2004. Rapid temporal modulation of synchrony by competition in cortical interneuron networks. *Neural Computat.*, **16**, 251–275.

Traub, R. D., Whittington, M. A., Colling, S. B., Buzsaki, G., & Jefferys, J. G. 1996. Analysis of gamma rhythms in the rat hippocampus *in vitro* and *in vivo*. *J Physiol*, **493**, 471–484.

van Vreeswijk, C., Abbott, L. F., & Ermentrout, G. B. 1994. When inhibition not excitation synchronizes neural firing. *Journal of Computational Neuroscience*, **1**, 313–322.

Vanderwolf, C. H. 1969. Hippocamapal electrical activity and voluntary movement in the rat. *Clin. Neurophysiol.*, **26**, 407–418.

Wang, X.-J., & Buzsáki, G. 1996. Gamma oscillations by synaptic inhibition in an interneuronal network model. *J. Neurosci.*, **16**, 6402–6413.

Wang, X.-J., & Rinzel, J. 1992. Alternating and synchronous rhythms in reciprocally inhibitory model neurons. *Neural Computat.*, **4**, 84–97.

White, J., Kopell, N., Banks, M., & Pearce, R. 2000a. Fast and slow $GABA_A$ networks of interneurons provide substrate for mixed gamma-theta rhythm. *Proc. Natl. Acad. Sci. USA*, **97**, 8128–8133.

White, J. A., Chow, C. C., Ritt, J., Soto-Treviño, C., & Kopell, N. 1998. Synchronization and oscillatory dynamics in heterogeneous, mutually inhibitory networks. *Journal of Computational Neuroscience*, **5**, 5–16.

White, J. A., Banks, M. I., Pearce, R. A., & Kopell, N. 2000b. Networks of interneurons with fast and slow gamma-aminobutyric acid type A (GABAA) kinetics provide substrate for mixed gamma-theta rhythm. *Proc. Natl. Acad. Sci. USA*, **97**, 8128–8133.

Whittington, M. A., & Traub, R. D. 2003. Interneuron Diversity series: Inhibitory interneurons and network oscillations in vitro. *Trends Neurosci.*, **26**, 676–682.

Williams, J. H., & Kauer, J. A. 1997. Properties of carbachol-induced oscillatory activity in rat hippocampus. *J. Neurophysiol.*, **78**, 2631–2640.

List of Figures

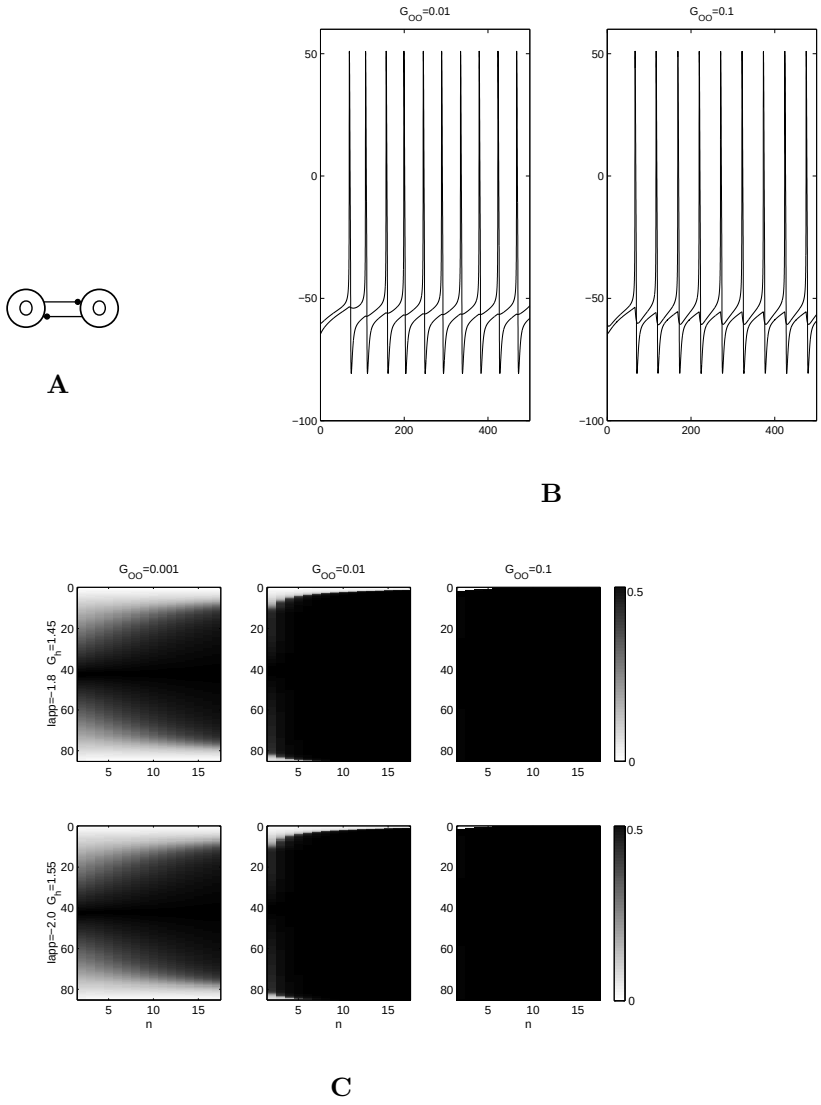

Figure 1:

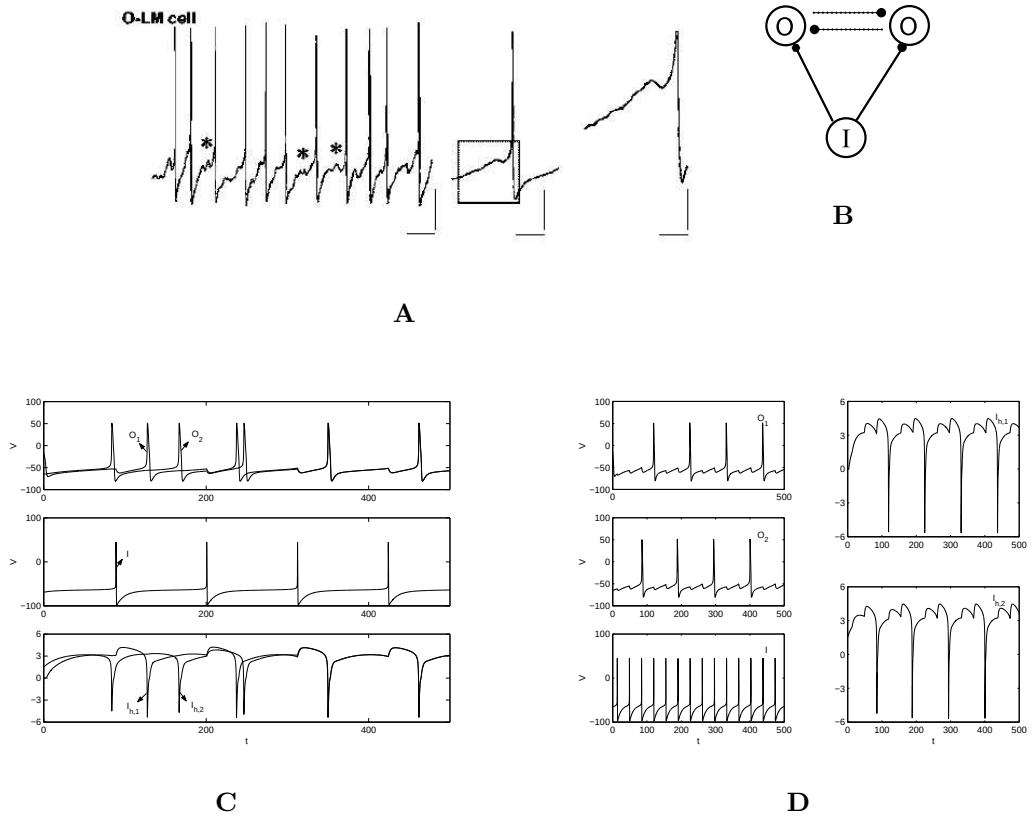

Figure 2:

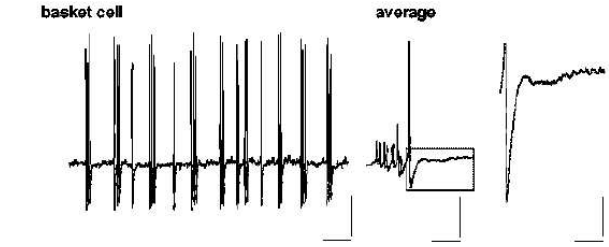

A

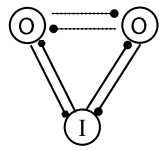

B

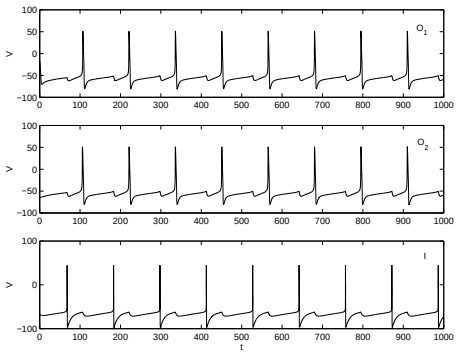

C

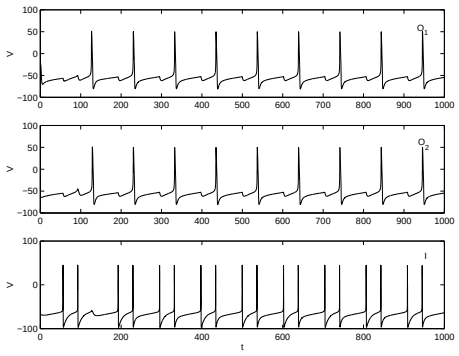

D

Figure 3:

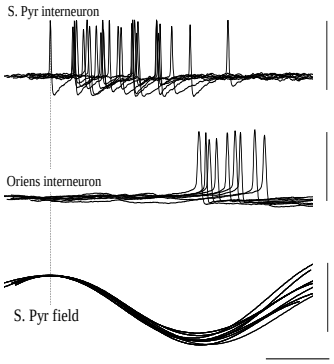

A

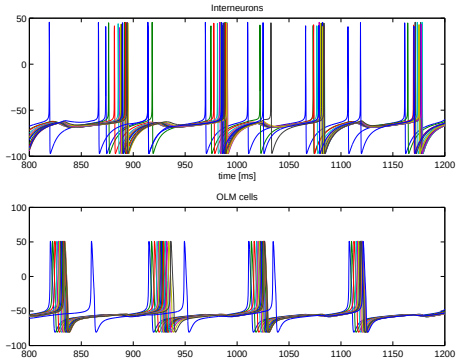

B

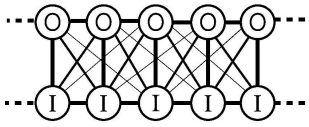

C

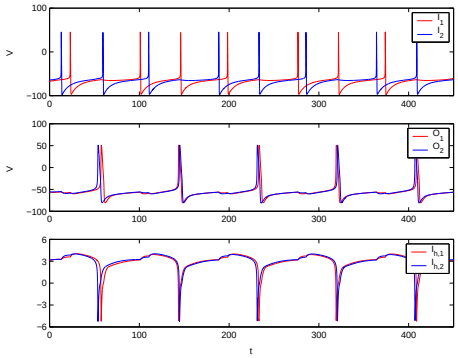

D

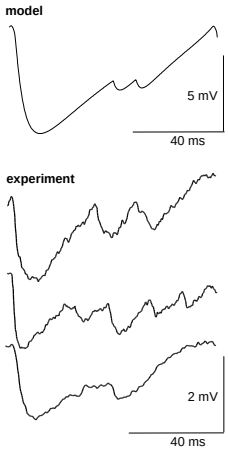

E

Figure 4: